Single-Plane Balancing of A Rotor Directly Coupled to An Induction Motor by Using Residual Current Data.

Alfonso C. García Reynoso[1,2], Enrique Ladrón de Guevara Durán[1,2], Alfonso García Portilla[1], Alberto P. Lorandi Medina[2], Guillermo Hermida Saba[2]

[1]Instituto Tecnológico de Veracruz, Miguel Ángel de Quevedo 2779,
C.P. 91860, Veracruz, Ver. México. Tel. y Fax (52) (229) 9385764.

[2]Instituto de Ingeniería de la Universidad Veracruzana, Juan Pablo II s/n Boca del Río,
Veracruz, C.P. 94294 México. Tel. y Fax (52) (229) 7752000 ext. 22214

This research was supported by Dirección General de Educación Superior Tecnológica awarded to Alfonso C. García Reynoso.

Correspondence concerning this article should be addressed to:
Alfonso C. García Reynoso,
Avenida Costa Verde 832, CP 94294 Boca del Río,
Veracruz, México.
E-mail: algarcia@uv.mx

Abstract

A method for single-plane rotor balancing which requires some components of the electric signal spectrum from each phase of the electric motor to which it is directly coupled is developed. The signal readings show a residual complex value (offset) when there is no imbalance, and this causes a nonlinear behavior of the data with respect to the unbalance forces, thus requiring an algorithm to subtract the offset, and to obtain the phase for the test data. Furthermore, the influence coefficients and balancing masses are calculated. This algorithm was verified by running two study cases, with satisfactory results.

Keywords: Single Plane Balancing, Induction Motors, Current Harmonics.

Nomenclature

F_0 : Original unbalance force at work radius

F_2 : Force produced by original unbalance plus the trial weight 2

F_4 : Force produced by original unbalance plus the trial weight 4

F_6 : Force produced by original unbalance plus the trial weight 6

W_{p_2} : Trial weight 2

W_{p_4} : Trial weight 4

W_{p_6} : Trial weight 6

N : Measured current, milliamp, original unbalance

N_2 : Measured current, milliamp with trial weight 2

N_4 : Measured current, milliamp with trial weight 4

N_6 : Measured current, milliamp with trial weight 6

θ_i : Phase angle

1. Introduction

The relationship among the spectral harmonics of an electric current induction motor, and its mechanical and electromagnetic problems is well known. Dorrel (1995) studied how the magnitude of electric harmonics relates to the mechanical harmonics in motors focusing on eccentricity.

(Riley, Lin, Habetler & Kliman, 1997; Riley, Lin & Habetler, 1998; Riley, Lin & Habetler, 1999) analyzed these relations to establish limits for the electric harmonics as they correlate with vibrations, concluding there is a monotone relationship between these two variables. Caryn (1997) finds, based on theoretical as well as on experimental bases, that there is a linear relationship between specific electric harmonics and mechanical vibration. Additionally, Caryn (1999) presents an analysis including the effect of externally induced vibrations. Finley (2000) makes a complete analysis of the relation among electric harmonics and mechanical problems including misalignment, unbalance, bearings failure, fractured rotor bars, etc. Kral (2004) proposes a technique to estimate unbalance using harmonics that are present in the electric power, showing positive results in assessing static and dynamic unbalance. Neelam (2007) presents an analysis of the electric current as the most popular for failure diagnosis not only electrical but mechanical as well showing effectiveness to determine abnormal operation of induction motors, including situations involving gear trains. Bellini (2008) presents a paper review of the previous ten years showing a list of references and research activity classified in four topics: a) electric failures, b) mechanical failures, c) signal processing for monitoring and analysis, and d) technical decision using artificial intelligence. Camargo (2009) presents results of single-plane rotor balancing using electric harmonics that relate to mechanical unbalance.

2. Measurement of residual current signals

A residual current is considered as the remaining harmonics after subtracting the fundamental current circulating in a motor wiring. These harmonics are due to different effects, mechanical and electrical, as has been reported for some time (Finley, Hodowanec & Holter, 2000; Bellini, Filippeti, Tassoni & Capolino, 2008).

These currents are produced by a deformation of the magnetic field in the motor air-gap, as a result of mechanical unbalance. However, the residual condition is also obtained by motor eccentricity, asymmetry of coil structure of stator and rotor, that is, due to static and dynamic irregularities in the air-gap (Riley, Lin, Habetler & Kliman, 1997; Finley; Bellini, Filippeti, Tassoni & Capolino, 2008).

By means of the sensing system, the fundamental current consumed by the motor, and the harmonics produced by the mechanical and the electromagnetic problems are obtained. The Fourier spectrum of the signal is displayed and the mechanical unbalance is indirectly determined by filtering the associate harmonics.

The measurement system is formed by a virtual instrument, a set of sensors and its signal conditioning.

The virtual instrument is developed using Labview 8.6 @ from National Instruments. The sensing and conditioning systems are built for a three-phase system, with a capacity to work with a 220 volt input, 15 Amperes. The voltage signal is monitored through transformers connected in a star configuration, whose magnetic cores respond to a maximum of 10 kHz. The electric signal is obtained through Hall-effect sensors model M15 with the capacity to measure direct and alternating components up to 10 kHz.
The virtual instrument may employ two data acquisition cards, the NI USB 6009, and the NI USB 9233. This instrument is configured to capture two harmonics that relate to mechanical unbalance, that depend on the rotor slip, input frequency, and they occur at the frequencies h_1 and h_2 given by the following expressions:

$$h_1 = f_s + f_r \quad (1)$$

$$h_2 = f_s - f_r \quad (2)$$

Where:

f_r : Rotor angular velocity in revolutions per second

f_s : Line frequency of motor

h : Harmonic frequency that relates to the mechanical unbalance

Once the harmonic frequencies are obtained, the signal is filtered with an IIR filter with a similar configuration to the Butterworth analog filter to obtain a more precise behavior of these harmonics.
This instrument was validated with commercial ammeters, and calibration was performed through an electronic circuit that conditions the signal using software.
The measurement system is of low cost, and the data acquisition card is simple. It connects to a laptop computer with Lab-view.
During the tests, measurements were taken in five-minute samples for each run. The kind of signal is shown in time in figure 1. As it may be seen, signal has large variations, and that makes it necessary to use the root mean square (RMS) to get a representative value.

3. Characteristics of the spectral values of electric current

Due to the fact that harmonic magnitudes do not converge to zero for a balanced rotor, as mechanical vibrations do, they show an offset which may be different for the three current lines. When unbalance is present, the measured values of harmonics do not follow a linear relationship with the unbalance forces. However, after the offset is removed, the relation is approximately linear as shown in figure 2 for a test case. In this figure, the lower curve has the offset removed (as will be described below), and it tends towards the origin as the unbalance tends to zero. This corrected curve is nearly linear and homogeneous, as is mechanical unbalance.
The subtraction process of the offset requires knowing the phase (complex values) of the harmonics, which in these measurements is not determined. This process is numerical as described below.

4. Rotor balancing formulas

The rotor inertia forces when trial weights are used are composed of the original unbalance force plus the centrifugal force due to the trial weight. These expressions are:

$$F_2 = F_0 + W_{p2} \quad (3)$$

$$F_4 = F_0 + W_{p4} \quad (4)$$

$$F_6 = F_0 + W_{p6} \quad (5)$$

By relating the inertia forces with the corresponding responses after subtracting the offset the following equations are obtained, where each quantity is complex. This corresponds to one of the three lines Li.

$$\frac{N - O_f}{N_2 - O_f} = \frac{F_0}{F_2} \quad (6)$$

$$\frac{N - O_f}{N_4 - O_f} = \frac{F_0}{F_4} \quad (7)$$

$$\frac{N - O_f}{N_6 - O_f} = \frac{F_0}{F_6} \quad (8)$$

From here, three expressions for the offset are obtained:

$$O_f = \frac{N_2 F_0 - N F_2}{F_0 - F_2} \quad (9)$$

$$O_f = \frac{N_4 F_0 - N F_4}{F_0 - F_4} \quad (10)$$

$$O_f = \frac{N_6 F_0 - N F_6}{F_0 - F_6} \quad (11)$$

Let the following relation of inertia forces be

$$a = \frac{F_0}{F_6} \quad (12)$$

$$b = \frac{F_0}{F_4} \quad (13)$$

$$c = \frac{F_0}{F_2} \quad (14)$$

Dividing the right side of equation (11) by F_6 and substitution of (12) gives:

$$O_f = \frac{a N_6 - N}{a - 1} \quad (15)$$

Similarly:

$$O_f = \frac{b N_4 - N}{b - 1} \quad (16)$$

$$O_f = \frac{c N_2 - N}{c - 1} \quad (17)$$

Now take the complex conjugate of (15) to obtain:

$$O_f^* = \frac{a^* N_6^* - N^*}{a^* - 1} \quad (18)$$

Multiplying side to side (15) times (18) gives:

$$\left|O_f\right|^2 = \frac{\left|a N_6\right|^2 + \left|N\right|^2 - 2\mathrm{Re}\left\{a N_6 N^*\right\}}{\left|a\right|^2 + 1 - 2\mathrm{Re}\left\{a\right\}} \quad (19)$$

The real part of this equation is:

$$\mathrm{Re}\left\{a N_6 N^*\right\} = \frac{1}{2}\left[-\left|O_f\right|^2\left(\left|a\right|^2 + 1 - 2\mathrm{Re}\left\{a\right\}\right) + \left|a N_6\right|^2 + \left|N\right|^2\right] \quad (20)$$

Dividing the real part by the absolute value, a cosine is obtained:

$$\cos(\theta_a + \theta_{N_6} - \theta_N) = \frac{\mathrm{Re}\{aN_6N^*\}}{|aN_6N^*|} \quad (21)$$

From this equation, the phase θ_{N_6} is obtained assuming that phase θ_a is known, and phase θ_N is assumed zero as an arbitrary reference.

Similarly, the following expressions are obtained:

$$\mathrm{Re}\{bN_4N^*\} = \frac{1}{2}\left[-|O_f|^2\left(|b|^2 + 1 - 2\mathrm{Re}\{b\}\right) + |bN_4|^2 + |N|^2\right] \quad (22)$$

$$\mathrm{Re}\{cN_2N^*\} = \frac{1}{2}\left[-|O_f|^2\left(|c|^2 + 1 - 2\mathrm{Re}\{c\}\right) + |cN_2|^2 + |N|^2\right] \quad (23)$$

From these formulas, phases θ_{N2} and θ_{N4} are obtained.

Having determined the harmonic phases, it is possible to calculate the influence coefficients as well as the balance masses for each combination of trial weights. In the traditional method of influence coefficients formulas (24) and (27) provide a balance mass assuming the magnitude and phase are known. This may be extended if more test runs are conducted.

$$A_2 = \frac{N_2 - N}{W_{p_2}} \quad (24)$$

$$A_4 = \frac{N_4 - N}{W_{p_4}} \quad (25)$$

$$A_6 = \frac{N_6 - N}{W_{p_6}} \quad (26)$$

$$W_{c_2} = -\frac{N}{A_2} \quad (27)$$

$$W_{c_4} = -\frac{N}{A_4} \quad (28)$$

$$W_{c_6} = -\frac{N}{A_6} \quad (29)$$

The average of balance masses is:

$$W_{prom} = \left(W_{c_2} + W_{c_4} + W_{c_6}\right)/3 \quad (30)$$

5. Proposed balance method

The numerical procedure is the following, for each of the three lines L_i:

1. An initial parameter value of F_0 is established. This may be estimated according to the vibration level observed, by giving a value between the tolerance value as given by the ISO balance standards and the maximum which would be twenty times as much for a severe unbalance.
2. The inertia forces F_2, F_4 y F_6 and the quotients, *a, b* and *c* are calculated according to the equations (3) to (5) and (12) to (14).
3. Applying equations (20) to (23), each harmonic phase is determined.
4. Influence coefficients and balance masses are obtained for each combination of test runs. This is done from formulas (24) to (30).
5. The average of the balance masses will have a difference with the supposed initial parameter F_0, and a new parameter is defined by taking the last estimate, and the process iterates to step one. This is

repeated until a minimum difference between the parameter F_0 and the average balance mass is obtained.

6. Applications

The first test was run on an induction motor with the characteristics shown in table 1. In order to set a rotor unbalance, a mass of 8.7 g ∠0° was attached to a test rotor directly coupled to the motor. Then several test runs with the addition of trial weights as shown in tables 2 and 3 were conducted. Tables 2 and 3 give rms values of current spectrum for the test runs conducted. The first run corresponds to the original unbalance. The second test run is for trial weight W_{p_2} and the following two tests are for the trial weights W_{p4} and W_{p6}. The fifth run corresponds to the balanced rotor (no mass added). These tables show the amplitudes of the harmonics while their phases are obtained during the numerical process that follows.

The calculated balance masses are shown in table 4.

The balance mass expected is 8.70 g ∠180°. With the calculated mass of 8.53 g ∠196.4° attached to the rotor, vibration is reduced from 67.31 micron to 19.05 micron which is low enough according to the standards.

Another case conducted uses a different motor with data shown in table 5.

The unbalance mass attached to this rotor is 20 g ∠0° which produces a lightly strong vibration.

The trial weights used in the test runs and results are shown in tables 6 and 7.The expected value is 20 g ∠180°. The average values of 19.3 g ∠188.7° gives an approximation comparable to the traditional balancing method.

As an application of interest for industry, it is possible to keep in memory the influence coefficients related to the electric harmonics, and with the monitoring of these harmonics the actual balance mass at any given time may be known, based on the electric measurements.

7. Conclusions

1. Based on previous work of other researchers, where a relationship between the mechanical unbalance and the electric-current harmonics is reported, a method of balancing that uses the rms values of these harmonics is developed in this article.
2. This balancing technique faces two problems; one is that of data dispersion in each sample. This may be solved by taking three to five minute samplings, followed by the calculation of the rms value of the response. The other difficulty is the nonlinearity of data due to an offset.
3. The magnitudes of the signal spectrum do not have a linear relationship with the unbalance force due to a complex offset that can be measured with the balanced rotor, and that adds to the unbalance effects.
4. For the balanced rotor condition, the magnitude of the offset can be measured, but not its phase, which may be known through a calculation. These values change for each frequency line as well as for high or low harmonic frequency (h_1 or h_2).
5. For the trial-weight runs, phase is iteratively calculated, depending on the parameter F_0, which is the original equivalent unbalance.
6. The numerical process consists in establishing an initial value of the parameter F_0, then determining the phase for each line frequency, and then calculating the balance masses, one for each trial weight. The mass average will have a difference with the assumed parameter F_0, which defines a new parameter to continue iterating until a minimal difference is obtained.
7. The two test cases shown in this paper give balance masses that approach the expected values.

8. The virtual instrument, as developed in this project, is of low cost, and it may have some potential for industrial applications.

References

Bellini A., Filippeti F., Tassoni C., and Capolino G. A. (2008). Advances in Diagnostic Techniques for Induction Machines. IEEE Transactions on industrial electronics Vol. 55 No 12 Dec. 2008.

Camargo M. J, García R. A., Ladrón de Guevara D. E., Hernández M. E.. Balanceo dinámico de motores de inducción utilizando componentes de corriente eléctrica. XV Congreso Internacional Anual de la SOMIM, Instituto Tecnológico Superior de Cajeme, Cd. Obregón, Son., 23, 24 y 25 de septiembre, 2009, No. de registro: A4_21.

Dorrell D. G., W.T.Thomson, and S. Roach. (1995). Analysis of airgap flux, current and vibration signals as a function of the combination of static and dynamic airgap eccentricity in 3 phase induction motors. IAS 95 Conference record of the 1995 IEEE Industry applications Conference Vol. 1 pp 563-70, 1995.

Finley W, Hodowanec M., and Holter W. (2000). An analytical approach to solving motor vibration problems. IEEE Transaction on industry applications Vol. 36 No 5, Sep/Oct 2000.

Kral C., Haebetler T., and Harley R. (2004). Detection of mechanical imbalance of induction machines without spectral analysis of time domain signals. IEEE Transaction on industry applications Vol. 40 No 4, Jul/Aug 2004.

Neelam M., and Dahiya R. (2007). Motor current signature analysis and its applications in induction motor fault diagnosis. International Journal of systems applications, engineering & development. Vol. 2, Issue 1 2007.

Riley, C.M., Lin B.K., Habetler T.G and Kliman G.B. (1997). Stator current based sensorless vibration monitoring of induction motors. Applied power Electronics conference and exposition 1997, Vol. 1 pp 142-7, Feb 1997.

Riley C.M., Brian K. Lin, and Thomas G. Habetler. (1998). A method for sensorless online vibration monitoring of induction machines. IEEE transactions on industry applications, Vol. 34, No.6, november/december 1998.

Riley C.M., Brian K. Lin, and Thomas G. Habetler. (1999). Stator current Harmonics and their causal vibrations: A preliminary investigation of sensorless vibration Monitoring applications. IEEE Transaction on industry applications Vol. 35 No.1, January/February 1999.

Table 1

Test motor No.1

Three- phase Motor, open, NEMA B design SIEMENS
LCN – continuous service
Serial No. H93
Frame NEMA 56
Factor of service 1.25
Ambient temperature 40°C
Weight 7.9Kg
Volts 220YY / 440Y
Rod axis side 6203 ZZ
Rod opposite side 6203 ZZ

Type: IRA3 054-4YK31
C.P 0.5
Insulation CL NEMA B
Rpm 1730
Inc. Temp. 80°C
60Hz.
Amps. 2.1/1.1
Slots
Stator: 36
Rotor: 26

Table 2

Harmonic values of test runs, mA, low frequency h_2 **.**

Case	B^+ 30Hz		
	L_1	L_2	L_3
N (original)	8.3294	7.2504	3.8380
N_2 $W_{p_2} \angle 90°$	10.4921	7.4727	4.5209
N_4 $W_{p4} \angle 180°$	6.4541	4.3135	4.8428
N_6 $W_{p6} \angle 270°$	6.9687	8.5890	4.8644
Balanced rotor	4.4663	3.6975	3.1463

Table 3

Harmonic values of test runs, mA, high frequency h_1 **.**

Case	C^- 90 Hz		
	L_1	L_2	L_3
N (original)	37.542	37.735	24.911
N_2 $W_{p_2} \angle 90°$	41.433	37.935	22.644
N_4 $W_{p4} \angle 180°$	40.728	35.069	27.767
N_6 $W_{p6} \angle 270°$	33.022	40.351	31.552
Balanced Rotor	38.824	34.224	29.260

Table 4
Balance masses for each case.

Case	Wc
B_L_1	10.6 g ∠220.4°
B_L_2	10.0 g ∠180.8°
B_L_3	5.1 g ∠193.2°
C_L_1	8.2 g ∠180.8°
C_L_2	10.8 g ∠180.8°
C_L_3	9.3 g ∠220.4°
Average	8.53 g ∠196.4°

Table 5
Test motor No.2

High Efficiency Motor
C.P 1.00
Frame 143T
Class AISL: F
Hz 60
Bearing load side 6205-2ZJC3
Continuous Service
@ F.S. 1.0
Temp. Rise B A F.S: 1.15
(kW .746)
ENCL APG phases 3
Code K
Max Ambient Temp.: 40°C A 1000 MSNM
30°C AT 2280 MSNM
Opposite Side 6203-2ZJC3
Model BR26
Series: L05-BR26-M
Nominal efficiency η 82.5%
F.S 1.15
Design B
230v 3.00A 3.30A
460v 1.50A 1.60A
Lubrication: Grease
Temp. Rise
Minimal Efficiency guaranteed 80.0
Motores U.S. de México, S.A de C.V
Apodaca, N.L.
Made in México
417128-006

Table 6
Harmonic values of test runs, mA, low frequency h_2 **.**

Case		B^+ 30Hz		
		L_1	L_2	L_3
Original unbalance	N	14.1859	12.6603	10.4341
$W_{p_2} \angle 90°$	N_2	14.8042	13.6692	10.5197
$W_{p4} \angle 180°$	N_4	9.0866	9.4966	7.3542
$W_{p6} \angle 270°$	N_6	13.1867	12.1646	9.7935
Balanced rotor		6.7854	7.0290	5.6990

Table 7
Harmonic values of test runs, mA, high frequency h_1**.**

Case		C^- 90 Hz		
		L_1	L_2	L_3
Original unbalance	N	15.5931	14.6171	5.7185
$W_{p_2} \angle 90°$	N_2	13.6925	11.9857	5.0569
$W_{p4} \angle 180°$	N_4	17.4675	15.8294	7.5024
$W_{p6} \angle 270°$	N_6	14.1594	14.0456	6.7413
Balanced rotor		21.2113	18.1909	10.4302

Table 8
Balance masses for each case.

Case	Wc
B_L_1	15.8 g $\angle 190°$
B_L_2	18.2 g $\angle 194°$
B_L_3	16.7 g $\angle 187.2°$
C_L_1	28.3 g $\angle 186.8°$
C_L_2	12.4 g $\angle 201.6°$
C_L_3	25.6 g $\angle 206.8°$
Average	19.3 g $\angle 188.7°$

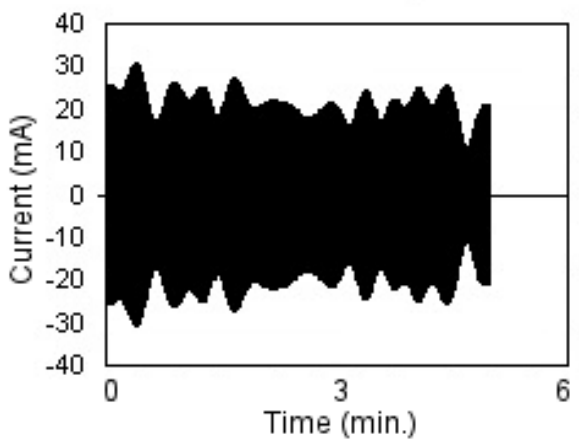

Figure 1. Time history of 90 Hz harmonic signal

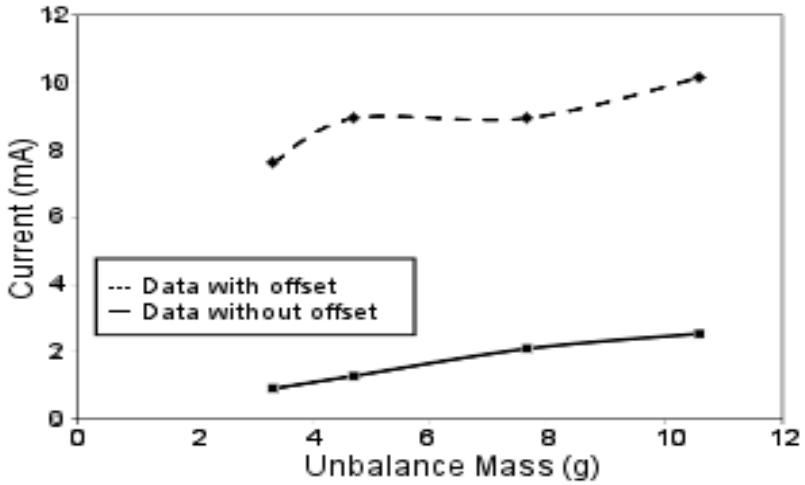

Figure 2. Behavior of harmonics with mechanical unbalance in grams.